

In presenting this dissertation as a partial fulfillment of the requirements for an advanced degree from the Georgia Institute of Technology, I agree that the library of the institution shall make it available for inspection and circulation in accordance with its regulations governing materials of this type.

I agree that permission to copy from, or to publish from, this dissertation may be granted by the professor under whose direction it was written, or, in his absence, by the dean of the Graduate Division when such copying or publication is solely for scholarly purposes and does not involve financial gain.

It is understood that copying from, or publication of, this dissertation which involves potential financial gain will not be allowed without written permission.

~~Marshall Fausold, Jr.~~ ✓

MODEL STUDIES OF PILE BEARING CAPACITY RELATIONSHIPS
IN A COHESIVE SOIL

A THESIS

Presented to
the Faculty of the Graduate Division
by
Howard Marshall Fausold, Jr.


In Partial Fulfillment
of the Requirements for the Degree
Master of Science in Civil Engineering

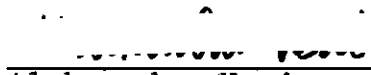
Georgia Institute of Technology
September, 1960


94
12R

MODEL STUDIES OF PILE BEARING CAPACITY RELATIONSHIPS
IN A COHESIVE SOIL

Approved:


George F. Sowers


Aleksandar Vesic


Radnor J. Paquette

Date Approved by Chairman: 8/29/60

ACKNOWLEDGMENTS

The writer wishes to express his appreciation to Professor George F. Sowers for the inspiration which led to this work and for his continued guidance throughout the entire project.

To Professors Aleksandar Vesic and Radnor J. Paquette thanks are extended for many helpful comments on the text.

TABLE OF CONTENTS

	Page
ACKNOWLEDGMENTS	ii
LIST OF TABLES	iv
LIST OF ILLUSTRATIONS	v
SUMMARY	vi
Chapter	
I. INTRODUCTION	1
II. THEORY	4
III. APPARATUS	9
IV. PROCEDURE	13
V. DISCUSSION OF TEST RESULTS	19
VI. CONCLUSIONS	28
VII. RECOMMENDATIONS	30
APPENDIX	31
BIBLIOGRAPHY	59

LIST OF TABLES

Table	Page
1. Square Pile Model--Forced Embedment (Data Sheet)	41
2. Square Pile Model--Buried Embedment (Data Sheet)	43
3. Square Pile Model--Forced Embedment (Load Distribution)	44
4. Square Pile Model--Buried Embedment (Load Distribution)	46
5. Round Pile Model--Forced Embedment (Data Sheet)	47
6. Round Pile Model--Buried Embedment (Data Sheet)	48
7. Round Pile Model--Forced Embedment (Load Distribution)	49
8. Round Pile Model--Buried Embedment (Load Distribution)	50
9. Plate Load Test Results	51
10. Summary of Soil Test Results	52
10a. Soil Properties Used in Calculations	52
11. Calculated Bearing Capacities	53
12. Comparative Bearing Capacities	55
13. Average Efficiency	57
14. Residual Side Friction	57
15. Measured Skin Friction	58
16. Modification of Bearing Capacities of Round Piles (Forced) to Compare with Standard Depth .	58

LIST OF ILLUSTRATIONS

Figure		Page
1.	Pile Load Distribution: Square, Forced, 15" . .	32
2.	Pile Load Distribution: Square, Forced, 22" . .	32
3.	Pile Load Distribution: Square, Forced, 30" . .	33
4.	Pile Load Distribution: Square, Buried, 15" . .	33
5.	Pile Load Distribution: Square, Buried, 22" . .	34
6.	Pile Load Distribution: Square, Buried, 30" . .	34
7.	Pile Load Distribution: Round, Forced, 17" . .	35
8.	Pile Load Distribution: Round, Forced, 24" . .	35
9.	Pile Load Distribution: Round, Forced, 32" . .	36
10.	Pile Load Distribution: Round, Buried, 15" . .	36
11.	Pile Load Distribution: Round, Buried, 22" . .	37
12.	Pile Load Distribution: Round, Buried, 30" . .	37
13.	Deflection of Square Pile Model	38
14.	Deflection of Round Pile Model	38
15.	Plate Load Tests: Round and Square Bases . . .	39
16.	Diagram of Stress Measuring Device in Pile Base	40

SUMMARY

The purpose of this investigation was to investigate the relationships between the load carrying capacity of a pile by means of side friction and end bearing. This was accomplished by means of two model piles, one of cylindrical and the other of rectangular cross-section. These models contained in their base a proving ring to which was attached SR-4 electronic strain gauges. This provided a direct measurement of end bearing stress. The remaining share of the total load applied to the model was assigned to side bearing.

The two configurations of pile model were tested at various depths of embedment and also by two methods of installation, namely: forced embedment and buried embedment. The same soil material, a bentonite clay, was used throughout.

The results of the tests show that the bearing capacity of a pile in side friction is reduced after the moment of failure. A simultaneous rise in end bearing occurs as the value of stress carried in friction falls.

The comparison of tests of buried piles with those of embeded piles reveals that at the point of failure they develop a slightly higher coefficient of skin bearing, but a much lower value of end bearing.

When the models were forced or driven into the soil, the instruments recorded a persistent upward force on the base of the pile. This force is reduced as thixotropy occurs in the clay. It is counteracted by a negative coefficient of skin friction, and the value of this coefficient determines the magnitude of this force.

It was found that even a small load applied to the head of a friction pile has an immediate effect on the base of the pile. Although by far the greatest share of such a stress is received by the sides of the pile in friction, a small proportion is directly transmitted to the base, and is resisted by end bearing.

The tests also developed that both friction and end bearing stress increase in uniform increments throughout the application of load. This relationship ceases to exist when the failure of the pile is imminent.

A need for further testing of other phases of the inter-relation between skin bearing and end bearing is evident. Soil stresses below and around the pile and along the pile shaft itself require considerable attention. An accumulation of data of this type is a prerequisite to the development of a comprehensive theory of friction pile behavior.

CHAPTER I

INTRODUCTION

With the increased use of pile foundations resulting from today's larger and heavier structures, a need for a clearer understanding of the behavior of pile foundations has become evident. A sound conception of the manner in which piles of different characteristics behave during driving and how they subsequently transmit their load to the soil is an invaluable asset, and it is vitally necessary if any degree of precision is to be reached in the engineering design of such foundations.

It has long been recognized that two separate processes are involved in the transfer of pile loads into the surrounding soil. These are end bearing and skin friction. The former is the direct vertical resistance to further penetration of the soil beneath the tip of the pile, while the latter is the side resistance forces of the soil pressing against the sides of the pile. Most piles employ both means of transmitting their load, but the conditions under which a pile is placed determine which effect is dominant.

When piles are driven in a cohesive (clay) soil, the piles are generally considered to be skin bearing piles, or,

as they are more commonly called, friction piles. It should be noted that the term "skin bearing" includes both the forces of friction and of adhesion between the soil and the pile. A skin bearing pile is one on which the effects of end bearing on the pile are considered to be of relatively little effect when compared to the load bearing capacity provided by the shear of the soil along the sides. However, when a group of such piles is driven in sufficiently close proximity to one another, it has been shown that they act as a group. As such, they may have an appreciable end area, and thus the previously neglected value for end bearing may assume considerable importance. This is especially true since in such a group the skin bearing capacity is greatly reduced.

The purpose of this research is to investigate the behavior of piles in a cohesive soil which are constructed in such a manner as to be greatly influenced by both end bearing and side friction. The variable factors involved in the study were the shape of the pile, the depth of embedment and the effect of driving versus backfilling about a pile placed in an excavation. Particular attention was directed toward the proportion of the total load carried by the two sources of support as the pile was progressively loaded to failure.

All tests were conducted in an artificially prepared bed of cohesive soil. Such soil particles are surrounded by

relatively thick layers of adsorbed water. This gives soil of this type the ability to deform plastically without cracking.

CHAPTER II

THEORY

In order to evaluate the load bearing capacity of a pile, it is necessary to separate the two influences of side friction and end bearing. The end of the pile may be considered as a separate single footing. This footing, treated apart from all other factors, may then be considered to transfer its load into a cohesive soil by the same formula which applies to all footings placed below the surface of a cohesive soil. According to Meyerhoff (1), this is

$$Q_p = (cN_c + \gamma D)A \quad (1)$$

where Q_p denotes the load transmitted to the soil by the pile point

c	"	"	average value of cohesion at the pile point
N_c	"	"	bearing capacity factor
γ	"	"	unit weight of the soil
D	"	"	depth of the pile point at base
A	"	"	area of the pile point

Theoretical and experimental evidence indicates that the factor N_c is of the order of 9, and that the cohesion " c " is

the undrained shearing strength of the clay (2).

The transmission of the load by friction is expressed by

$$Q_s = mcS \quad (2)$$

where Q_s denotes the load transmitted to the soil by skin friction

c " " average value of the shear strength of the soil

m " " coefficient of adhesion

S " " surface area of contact

The coefficient of adhesion is employed when the adhesion between the side of the pile and the surrounding soil is less than the shear strength of the soil. Its value is then equal to or less than one.

The combination of these effects is simply

$$Q = Q_p + Q_s \quad (3)$$

Substituting Equation (1) and Equation (2), this becomes

$$Q = (cN_c + \gamma D)A + mcS \quad (4)$$

The settlement of the pile head is made up of pile shortening, plus soil deformation adjacent to the pile as the soil is dragged down by the pile, plus movement of the pile through the soil in case the shearing value of the soil

is exceeded.

Stress distributions along the piles are developed thus, according to Soloman (3):

Stress in the soil quickly increases from zero at the surface to a fairly constant value in homogeneous soil, the shearing value of the soil being its limit. This begins at the upper end and continues until sufficient resistance has been mobilized in an upper section of pile length shown as l_1 . The resultant pile shortening is denoted by ∇_1 . An increased load of $R_1 + R_2$ reduces the value of l_1 by $\nabla + \nabla_{12}$ and also causes a new hydrodynamic stress condition in the soil, which adjusts itself in the course of hours or days. In order to reach equilibrium again, soil in the length l_2 will also be stressed. The length l_2 will be shortened ∇_2 , and l_1 will be shortened by an additional amount ∇_{21} . The unit stress p_1 will be increased to p_2 . This process will be continued under successive increments of loading until the load reaches the tip.

A modification of this theory by Seed states that the distribution of load along a friction pile is associated with the relative stiffnesses of the pile and the surrounding soil. Because the soil will invariably deform more readily than the pile, all practical examples will result in a portion of the load being transmitted to the pile tip (4).

The static formula for friction pile bearing capacity is expressed (5) by the formula

$$f_u = R_u - R_t/A_s \quad (5)$$

where f_u = the ultimate skin bearing value in pounds per square foot

R_t = the amount of ultimate load carried on the tip, in pounds

A_s = the surface area of the pile acting in friction, in square feet

Skin bearing values depend on the type of soil, depth in ground, degree of natural consolidation and saturation, shape of pile, and sometimes on the time interval between driving and testing. Unit value of skin bearing for a pile in cohesive materials may be assumed as uniform for the entire embedded length, although some conflicting results have been published (6).

The unit value for skin friction for a pile in clay may vary widely for the same clay depending upon the method used in placing the pile. Driving may have remolded the soil to such an extent that the structure has broken down and the clay become more plastic around the pile. Therefore, because a certain type of pile has been tested to a given friction value in a particular soil, it does not follow that a pile placed by some other method would sustain an identical load, even if the period of re-gel were the same.

The shape of the pile affects the unit skin friction value. It has been found by tests in silty clay that the

skin friction value is larger per square foot for round than for square piles where the diameter of the round pile equals the side dimension of the square pile, the ratio being approximately four to three (7).

CHAPTER III

APPARATUS

Two model piles were constructed for the series of tests. The first was of aluminum sheet metal formed into a square pile 5.0 inches on a side, and 36.5 inches long. The shaft of the pile was left hollow, and was open at both ends.

The base of the pile was the heart of the measuring system (Fig. 16). It consisted of a metal proving ring 3.0 inches in diameter and 4.0 inches long. To one side of this was bolted a metal plate slightly smaller than the opening at the end of the shaft. This plate was then inserted into the end of the pile and was fastened rigidly to the sides of the pile shaft. The plate and proving ring were fastened in such a manner that a small portion of the perimeter of the proving ring extended beyond the base of the shaft. To this side of the ring, opposite the plate which connected the ring to the sides of the shaft, a second plate was fastened. This second plate was the same area and configuration as a cross-section of the pile shaft itself. Because of the slight projection of the proving ring, a gap of approximately one-eighth inch was left between the pile shaft and this plate, which acted as the base for the pile. This gap allowed the proving ring to deflect freely when an axial

load was applied to the base. In order to prevent moisture or clay from entering the interior of the pile through this gap, it was covered by a thin rubber membrane which was sealed with plastic adhesive tape.

Before installing the proving ring and plates in the base of the pile model, four Baldwin-Lima-Hamilton electronic strain gauges, type SR-4, were installed on the proving ring. Two of these were designed to act as strain measuring gauges and two as temperature compensating gauges. They were installed on opposite sides of the ring, and were wired into two separate systems so that they might act as a check upon one another. The wiring leads from these gauges were led through a small hole drilled in the upper plate and on up the shaft to the open top.

This proving ring was calibrated on a laboratory loading machine at stresses considerably in excess of those expected or subsequently encountered. Repeated tests on this machine resulted in identical load-strain curves for the strain gauges, which indicated good installation. Recalibration after several series of tests had been run conformed to the earlier results.

The second pile model was of steel sheet metal formed into a round pile 5.94 inches in diameter, and 36.5 inches long. This yielded a pile of approximately the same base area as the square model. As with the square model, the shaft of the round pile was merely a hollow shell, open at

both ends. The same proving ring was used, and the same manner of installation employed, except that round plates were substituted to conform to the different pile configuration.

Both piles were coated with a liquid plastic preparation which, on drying, formed a thin membrane over the surface of the pile. This served the triple purpose of protecting the interior of the pile from moisture which might injure the strain gauges, preventing contact of the corrosive clay material with the metal of the pile shaft, and also providing a uniform covering for both the steel and aluminum pile shafts, so that a uniform value of resistance between the pile shafts and the clay would prevail.

The soil selected for the tests was the same commercial bentonite which had been used in other research projects in the Soil Mechanics Laboratory of the Georgia Institute of Technology. It is a highly colloidal, sensitive plastic clay which, when mixed with water, forms a thixotropic gel and swells to several times its original volume. This gel of bentonite and water is highly sensitive but possesses the ability to re-gel after being remolded. This property is very desirable as it enables the same mass of clay to be used throughout a lengthy testing program. Further, the clay is ideally cohesive, and possesses no properties of internal friction.

The clay was contained in a corrugated steel cylinder

36 inches in diameter and 50 inches deep. At all times except during actual testing the top of the cylinder was kept covered by a polyethylene sheet to prevent escape of moisture.

Periodic tests of shear strength were made with a variety of apparatus. The principal results were obtained with a conventional vane shear rod. Other tests for comparison were made with metal plates coated in plastic, and with a small aluminum cylinder which was rotated after imbedment in the clay.

Loading of the piles was accomplished by means of a lever system which could be adjusted to various heights over the protruding portion of the pile. This permitted convenient and accurate application of axial loads in excess of three hundred pounds. A standard micrometer dial gauge was employed in making observations of the settlement of the pile under the applied load.

CHAPTER IV

PROCEDURE

The testing program was designed to include four separate series of tests with the two pile models. Specifically, these consisted of subjecting the models to loadings sufficient to produce pronounced and continuing deflection at each of three depths of embedment. The piles were placed in the ground either by forcing into the clay or by excavation of a pit into which the pile was placed. The load was provided by dead weights acting through a lever system. Strain gauge readings provided data on stress relationships between the pile shaft and base before driving and during and after the test.

From earlier tests by Martin, it was learned that the bentonite gel reformed and re-gelled thixotropically after a period of three days subsequent to being disturbed and remolded by the placing of a pile (8). Accordingly, once all preparation of equipment was complete, testing proceeded on a three-day cycle.

Before the pile was placed in contact with the soil, the wire leads to the proving ring mounted electronic strain gauges were connected to the strain measuring equipment, and the zero stress-strain reading verified. These leads were

not disturbed at any time during the series of similar tests, so that any variation in the readings obtained would reflect a genuine change in the forces acting at the base of the pile and not merely a difference in resistivity in a new wiring connection.

Driven piles.--The models which were to be considered as driven piles were forced into the bentonite by hand. When a penetration of several inches caused sufficient resistance to pushing, lead weights were added until the pile could again be forced downward. More weights were added until the pile had been pushed to the desired depth.

After the pile had been placed in this manner, the lead weights were unloaded and the pile was left undisturbed for the three-day period. The polyethylene cover was replaced to prevent moisture loss in the bentonite during this period.

Strain gauge readings were taken after driving was completed and again at the end of the three-day "setting-up" period, immediately before commencing the loading test itself. Also, before the test was commenced, a micrometer strain gauge was placed on the head of the pile to record settlement. On the head of the pile was placed a small flat steel plate which bore evenly on the upper edges of the pile shaft and transmitted the load to it without producing local buckling. A circular depression in the center of this plate restrained a 0.5 inch diameter ball bearing through which

the loading apparatus acted. This insured axial loading.

With all preparations completed, the lever arm of the loading apparatus was lowered gently onto the ball bearing. The weight of this loading apparatus constituted the first increment of load on the pile for this particular test. A reading was then made on the strain gauge equipment to discover the effect of this load on the base of the pile. A measurement of deflection was made on the micrometer strain gauge to determine the settlement of the pile under the loading increment.

When the three necessary measurements (two electronic strain gauge readings and the micrometer) had been obtained, a load weight was placed on a tray at the end of the lever arm. The loading was continued until a clear and pronounced failure of the pile occurred.

When the test was completed the loading apparatus was disassembled and removed. Readings of the strain gauges revealed the stress on the pile under zero load immediately subsequent to failure. The pile was then forced to a new depth by loading to rapid failure with lead placed directly on the pile. The strain gauges were reread after the new depth had been reached and the weights were removed. The pile was left undisturbed for the three-day period before the next test was begun.

The procedure outlined above was followed for both round and square piles when the series of tests intended

required forced or driven embedment of the pile model.

Buried piles.--When placed or buried embedment was called for, a pit was dug in the clay to a depth of approximately one pile diameter (or width) below the desired depth of embedment. The pit was backfilled until the bottom was the desired distance below the surface of the bentonite. The pile model was placed vertically in the pit, which was then backfilled around the pile. Loading and measuring methods were identical to those used in testing the driven piles. At the conclusion of the test the pile was excavated by hand and the pit deepened for the placing of the pile at the next desired depth.

In these tests a three-day waiting period was also employed after placing the pile to permit thixotropic hardening of the remolded clay. Since the end of the pile was under essentially zero load under this method of placement, no strain gauge readings were made at the start of the three-day period. In all other respects the same procedure for the test series was carried out as with the driven pile models.

Related tests.--Besides the principal pile model tests, a number of related tests were conducted. The end plates of both the round and square piles were placed on a bed of bentonite which had been remolded three days previously, and were loaded to failure in a standard plate load test. This determined the surface bearing capacity of a simple footing

of the same shape and area of the pile base.

A series of tests of various types was made to determine the frictional resistance of the bentonite to the plastic coated metal of the piles. Vane shear tests were made repeatedly to obtain both the undrained shear strength and the sensitivity of the soil. Metal plates of both steel and aluminum were coated with the liquid plastic and the frictional resistance to these as they were forced through the bentonite was measured. Finally, an aluminum tube of 1.25 inches diameter, which had itself been used as a pile model in a previous series of tests, was driven to a depth of one foot into the clay and, again after a three-day interval, rotated. The torque required to induce this rotation was used as an indication of side friction resistance.

Attempts were made during the course of this testing program to secure data of a related nature. Specifically, these were the values of soil pressure at various depths under the tip of the pile, and the stress versus depth of embedment along the pile shaft itself. The first was done by constructing pressure cells of aluminum containing electronic strain gauges and burying them under the spot where the tip of the pile would subsequently be placed. The results obtained from this were somewhat erratic and it was felt that an adequate evaluation was impossible with the limited data available, and that investigation of this field

should be the subject of a separate research project.

Measurements of stress along the pile shaft were also planned utilizing electronic strain gauges. This was attempted only on the round pile model. Because this was constructed of steel, it was necessary to concentrate the axial compressive stress in small areas so that sufficient strain would occur to register on the gauges. To accomplish this, the cylinder was cut in such a manner that it was connected at the third points by relatively narrow bands of metal. On these the strain gauges were placed. The cuts were kept extremely narrow so that the configuration of the pile was not altered. Data obtained here was very unsatisfactory, and it is felt that adequate investigation of this field must be done with a pile made of material of sufficiently low modulus of elasticity so that no artificial concentration of stresses is necessary.

CHAPTER V

DISCUSSION OF TEST RESULTS

The results of the testing program are diagrammed principally in a group of twelve graphs illustrating the relative behavior of the end and side resistances to each other and to the total load. These graphs are divided into four groups corresponding to the four series of tests run. Each group is preceded by data sheets containing the readings obtained during the tests, and by a tabulation of the loads and load distribution. Following the section containing the graphs is a group of tabulated computations of soil properties, theoretical bearing capacities, and relationships established between expected and actual results.

The tests resulted in the collection of considerable data on the behavior of a simulated pile loaded to failure in a sensitive cohesive soil. Particularly informative was the information gained on the relative behavior and bearing capacities of the end bearing and side bearing elements of the total strength of the pile.

The first series of tests was conducted with the square pile model under conditions of forced embedment. After the three-day "setting-up" period had elapsed, a residual compressive force on the base was indicated by the

measuring devices. This meant in effect that the forces of side friction were acting in opposition to an upward force on the pile base. This effect was observed in all cases where the pile was forced into the soil. Approximately the same magnitude of vertical forces was developed by both the square and round models at the various depths of embedment. This force increased with the depth to which the pile had been driven, but did not appear to increase so rapidly as greater depths were reached.

An examination of the values of skin bearing developed by this residual force (Table 8) shows that these values fall within a narrow range. (An exception is the value yielded by the round pile driven to 17 inches embedment. This pile provided a value considerably lower than any other in this case, as in several others.) This range of values was 0.214 psi to 0.265 psi, all negative. It is emphasized that this was at the end of the three-day waiting period after placing the pile, and that thixotropic action in the clay should have been nearly complete. This consistency in the effective skin friction over a range in depth of embedment and end bearing loads seems to indicate that it is the skin friction which determines the magnitude of this residual upward force.

When load testing of all of the pile models commenced, an immediate effect on the base of the pile was indicated by the electronic strain gauges. The end load

began to increase, showing a uniform increment of stress being supported by the base with each addition of load to the pile. However, the proportion of the total load on the pile which was transmitted to the base was very small in proportion to that received by the sides. This is illustrated by the graphs of total load versus end and side loads. (Figs. 1 through 6 and 7 through 12.) They show that the side loads increase much more rapidly than the end loads. They rise from a considerable negative value when the pile is unloaded at the start of the test to a value which is approximately equal to the end load as failure is reached. In contrast, the end load at the start of the test is already over 60 per cent of its final failure load.

These results are not compatible with the theory of Solomon (3), who claimed that no load was transmitted to the base until the side bearing had been fully developed. They do support the analysis of Seed (4), which concluded that differences in the elasticity of the pile material and the surrounding soil would permit immediate transference of a fraction of the load to the base. These pile models, with their much greater ratio of cross-sectional area to length, are much more sensitive to variations in end loads than a more conventional slender pile. The much lower rate of increase of the end load relative to the side load indicates that Solomon's approach is essentially applicable even in this case.

In all cases the graph illustrating the variation in distribution of load between the sides and base followed a straight line until the region of failure stress was approached. It might have been expected that since the base was receiving a portion of the load from the very first increment, the share of the total transmitted to the base might increase as the loading progressed, and a curve concave upwards develop. This was not the case in any of the tests, however.

A rapid variation in this relationship between the end and side resistances with respect to the total load occurred as the pile stress approached failure. The curve of end bearing showed a rapid increase in value and assumed a nearly vertical slope. This indicated that all, or almost all, additional load placed on the pile after the moment of failure is received at the base of the pile. Indeed, in most cases the proportion of the load supported by the side friction was actually reduced at failure, since a sharp drop was indicated at this point on the graph of side friction versus total load.

This failure appeared to be a sudden "semi-release" by the restraining skin friction and may be ascribed to the nature of the highly sensitive bentonite, which loses considerable strength upon remolding. In the case of the square pile buried at 15 inches, the pile was continued at a load in excess of failure, and the curve of skin friction

appeared to approach a constant value.

It was observed that the method of placement of the piles resulted in considerable difference in the relationship of the two factors involved in bearing capacity. Placing the pile by burying (Figs. 4 through 6 and 10 through 12) rather than by driving (Figs. 1 through 3 and 7 through 9) had the effect that instead of a considerable residual upward force on the base and a resulting negative action of the skin friction, both of these forces were at zero when no load was applied to the pile. As noted earlier, the value of the skin friction's share of the total load increased much more rapidly than that of the end bearing. Since both were beginning from zero, this meant that in the buried piles, skin friction carried a much larger share of the total load than was the case with the driven piles.

It seems obvious that skin friction entirely controlled the behavior of these pile models when they were placed by burying. In no case did the end load at failure for a buried pile, either round or square, exceed 21 per cent of the calculated theoretical value. In fact, the average of the six buried tests was only 12.5 per cent of that value. In contrast, the piles embeded by driving developed an end failure load of up to 64 per cent of the theoretical value, for an average of 52.5 per cent.

Also in support of this contention is the observation that the coefficients of skin friction developed by the

buried piles fall in a much narrower range than those developed by the driven piles (Table 14). The lowest value obtained for a buried pile was 0.328 psi and the highest was 0.419 psi. In contrast, the driven piles developed coefficients ranging from 0.214 psi to 0.396 psi, a spread exactly twice as great. Further, the average coefficient of skin friction was more than 27 per cent greater for buried piles than for driven ones.

Despite the higher values of skin friction for the buried models, their total bearing capacity was markedly lower than for the driven piles (Table 11). This resulted from the much higher end bearing of the driven piles which more than made up for their lower side friction. There was no exception to this characteristic, either. In no case did the buried pile exceed 98 per cent of the equivalent driven pile, and the average was 90 per cent for the square piles and only 67 per cent for the round piles, although the results for the latter are not strictly comparable since the driven piles were embedded to a depth of two inches greater than the buried piles. If a direct comparison is made by subtracting the bearing capacity provided by these additional two inches acting in skin bearing, the average is still only 70 per cent for the round piles (Table 15).

There was no exception to the pattern of stress relationships at failure. Regardless of the shape of the pile, the method of embedment, or the depth of embedment, the

approach of failure was indicated by a short period in which the end bearing assumed a greater and greater share of the additional increments of total load and the side friction less and less until the side friction suddenly dropped off and end bearing received all of the additional load.

The most unexpected result of the tests was the very low value of skin friction developed (Table 10). Vane shear measurements made after the tests developed an average value of 0.950 psi. It was realized that the coefficient of friction between the plastic coated pile shaft and the clay would be lower than this, and would therefore control the amount of load carried in friction. Other attempts to obtain a value of the frictional coefficient between the bentonite and the pile shaft were made. Thin metal plates coated with the plastic produced an apparent average coefficient of 0.885 psi when forced through the clay. This was still greater than the measured value in the pile tests by a factor of 2.66. A cylindrical aluminum tube embeded in the bentonite to a depth of one foot and subjected to a torque produced a shear strength value of 0.705 psi, or 2.12 times the actual average value and 1.68 times the highest value of skin friction obtained during the pile tests.

One explanation which can be offered is that the methods used to evaluate the skin friction independently of the actual tests were very inaccurate. The metal plates, although thin, nevertheless presented an appreciable end

area which undoubtedly affected the results obtained from them. The apparatus used to apply a torque to the aluminum tube also resulted in a lateral load which probably induced an error, although this seems to hold the promise of being the most accurate means of evaluating the frictional coefficient. Still another source of error lies in the difference in relative strain between the pile and the soil.

A major factor to this low apparent value of skin bearing was probably a progressive failure as outlined by Wilson (9). In such a case, friction developed along a pile shaft does not reach a constant value, but becomes greater with increasing depth. A sharp increase occurs near the bottom of the pile just prior to failure. Failure then first commences at the tip of the pile. Should this have been the case, the full theoretical skin bearing would never have been developed along the entire pile shaft at any one instant, and a resulting low value of apparent skin bearing would be noted.

The consistent nature of the values obtained for the coefficient of friction between the pile and the bentonite (excluding the results of the round pile driven to 17 inches which is much lower than any other) indicate that these are effective values (Table 14). They showed no significant variation with depth of embedment, although the lowest value in each series was obtained at the least depth of embedment, including the extremely low reading cited above.

The values obtained in end bearing were also much below those predicted by the Meyerhoff analysis (1). It is believed that the extremely sensitive nature of the bentonite is principally responsible here also. Tests with the vane shear apparatus revealed that the bentonite used in these tests had a sensitivity value of approximately 2, which means that its remolded strength was only one half of its undisturbed strength.

CHAPTER VI

CONCLUSIONS

1. An upward force of appreciable magnitude affects the base of a driven pile in a cohesive soil for some time after driving. As thixotropy progresses, its magnitude is reduced. However, it may persevere long after the soil has appeared to have re-gelled completely. It is counteracted by a negative value of skin friction. The value of this skin friction resistance to the vertical heave determines the magnitude of the force.

2. Even a small load applied to the head of a friction pile has an immediate effect on the base of the pile. Although by far the greatest share of such a stress is received by the sides of the pile in friction, a small proportion is directly transmitted to the base, and resisted by end bearing.

3. Both friction stress on the sides of the pile and end bearing stress on the base increase in uniform increments throughout the application of load. This relationship ceases to exist when the failure of the pile is imminent.

4. The capacity of the pile in friction is reduced after the moment of failure. Shortly before failure, a greater and greater share of each additional increment of

load is received in end bearing, while less is ascribed to frictional resistance. After failure, the total stress of skin friction is never as high as the peak value reached at failure.

5. A pile placed by burying in soil which has been remolded below the base as well as about the sides of the pile will develop only a fraction of the theoretical end bearing capacity before the maximum value of side friction is reached and the pile fails.

CHAPTER VII

RECOMMENDATIONS

1. Efforts should be directed towards an investigation of the distribution of friction stress along a pile. These investigations should attempt to relate variation in this distribution with variation in load below failure stress.

2. Investigation of soil stresses in the vicinity of a friction pile should be pursued. The pressure cell employing electronic strain gauges holds promise for this field, but problems involving sensitivity and moisture proofing will be encountered, as will problems in accurate location of the cells when the piles are to be driven.

3. A more accurate method of evaluating frictional coefficients should be devised. Perhaps the best would be a smooth cylindrical tube to which a torque wrench can be applied so as to provide a torque without inducing a lateral load.

A P P E N D I X

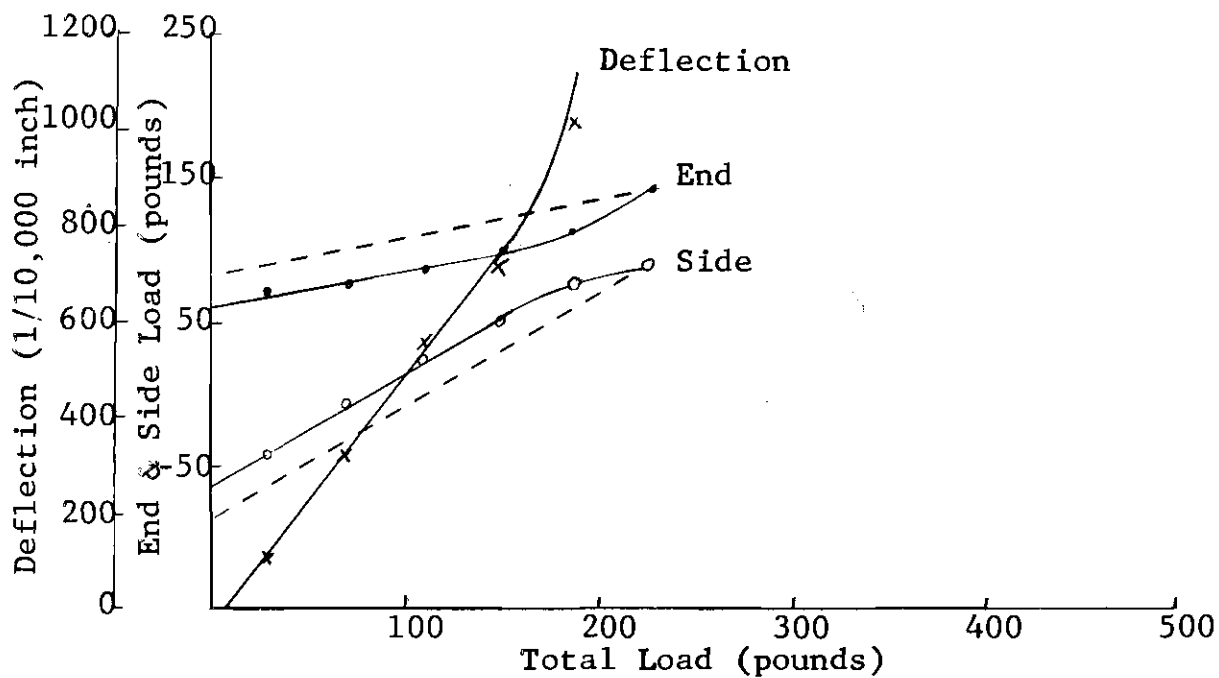


Fig. 1. Pile Load Distribution: Square, Forced, 15"

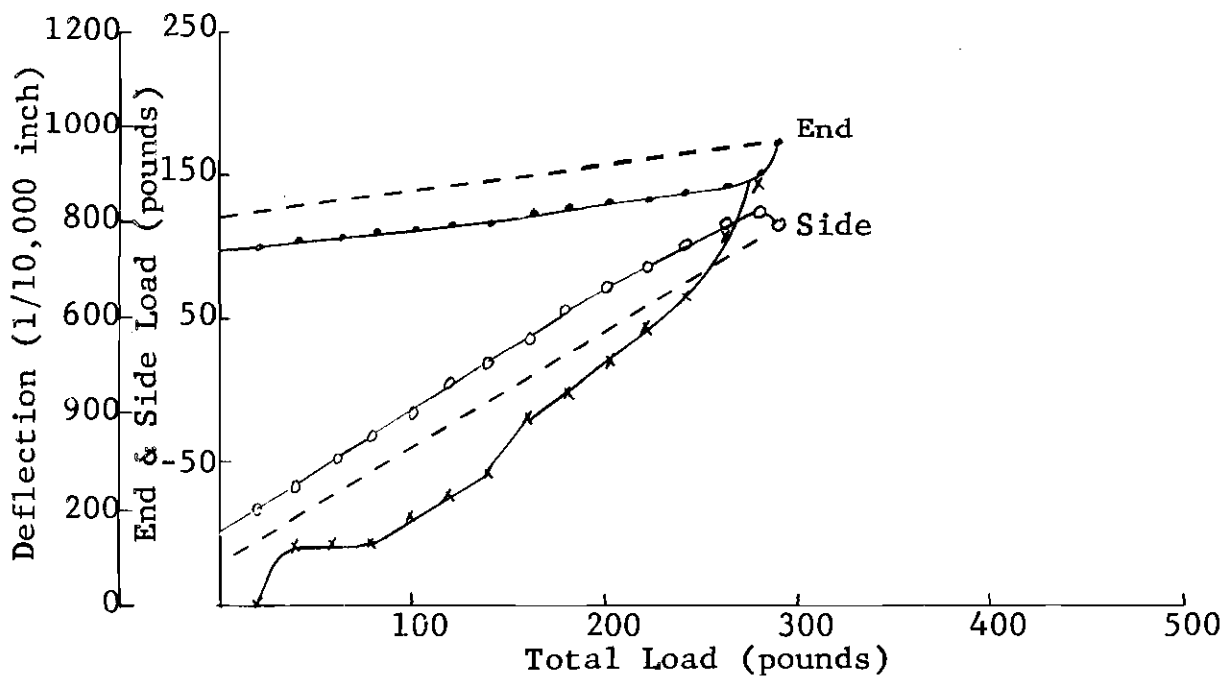


Fig. 2. Pile Load Distribution: Square, Forced, 22"

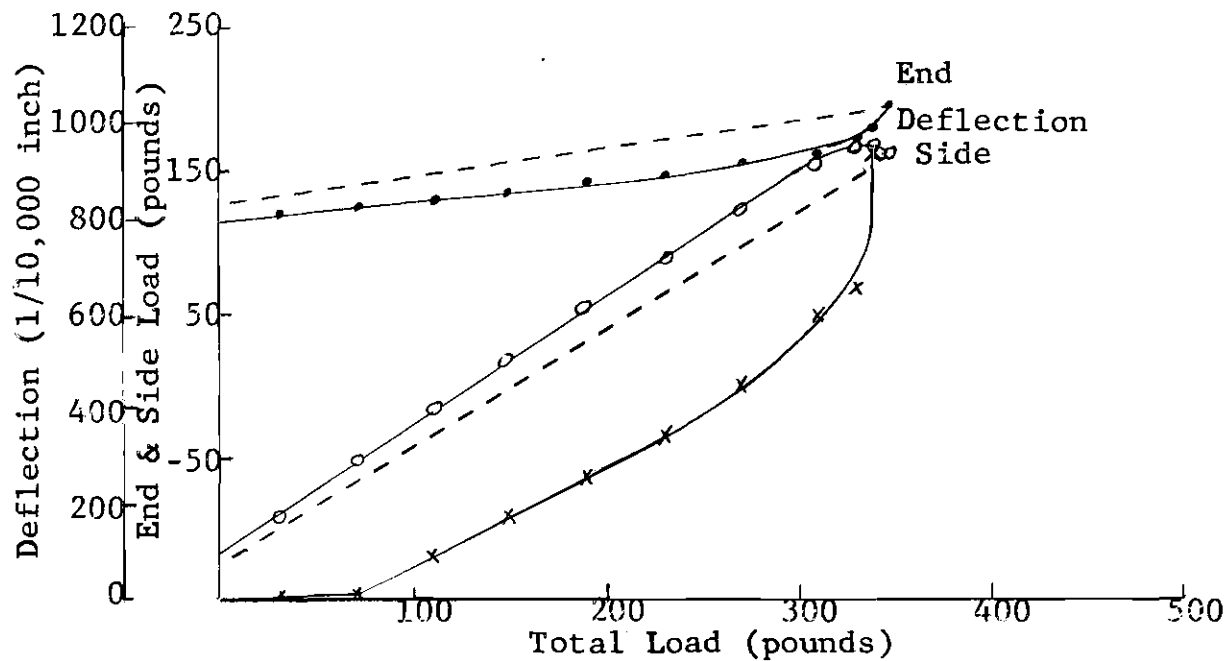


Fig. 3. Pile Load Distribution: Square, Forced, 30"

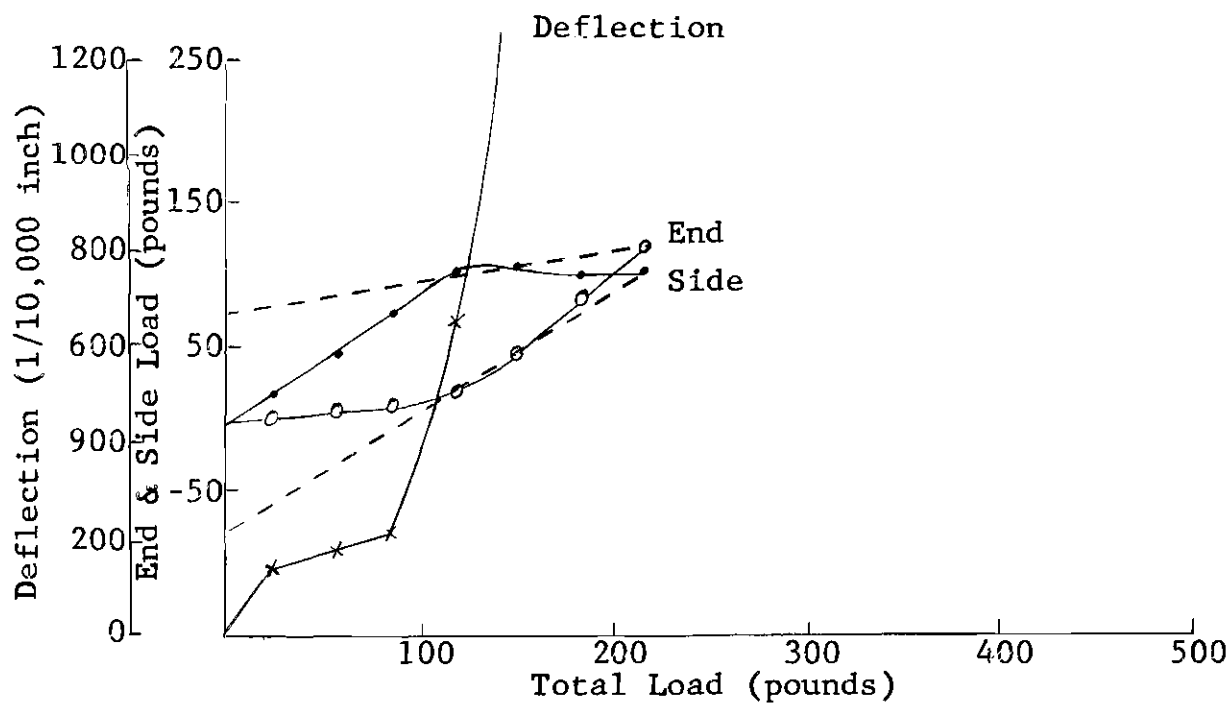


Fig. 4. Pile Load Distribution: Square, Buried, 15"

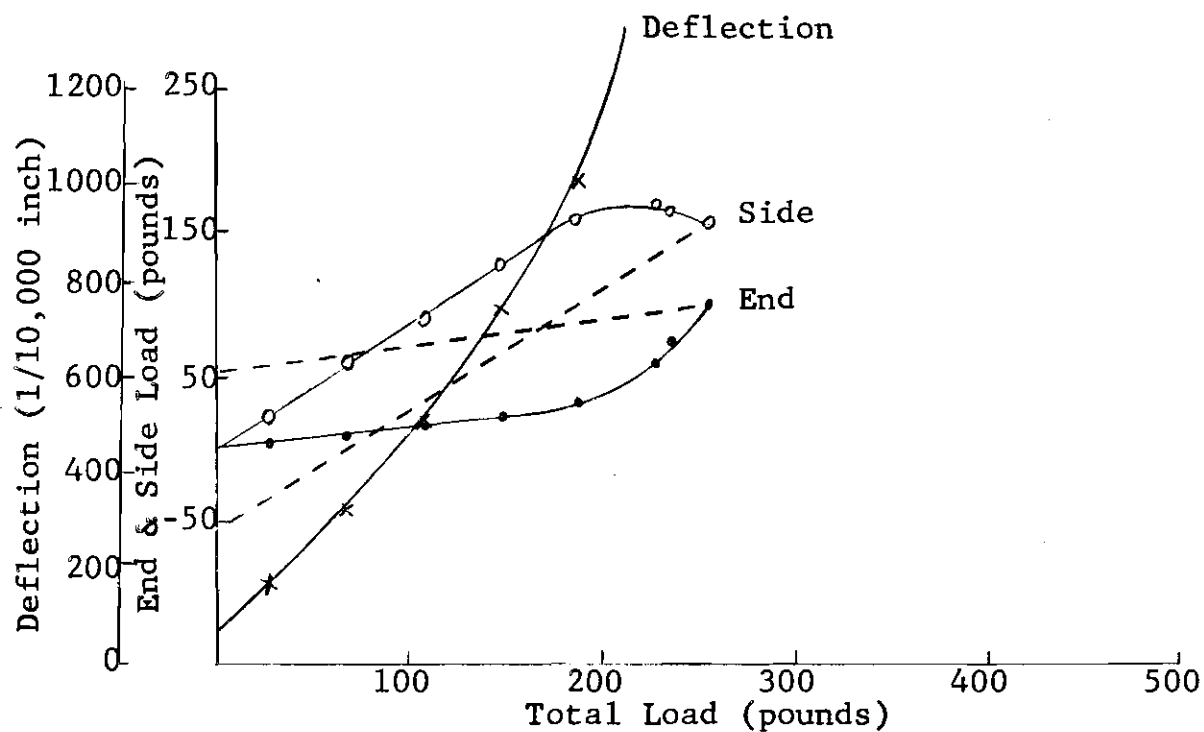


Fig. 5. Pile Load Distribution: Square, Buried, 22"

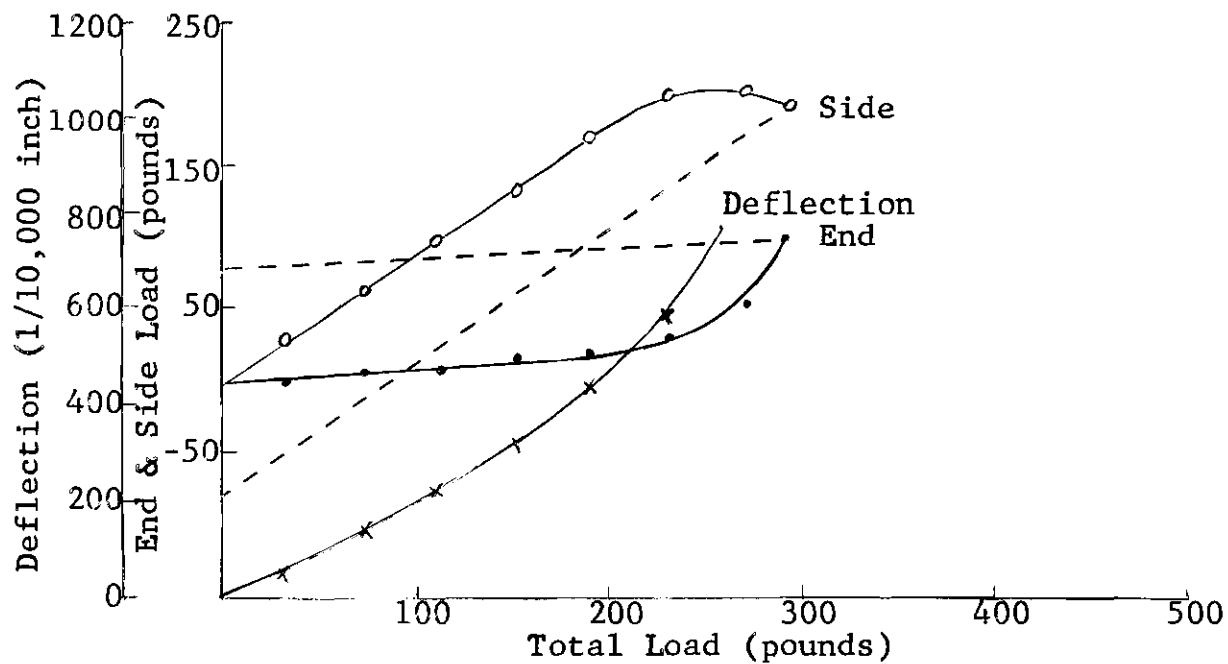


Fig. 6. Pile Load Distribution: Square, Buried, 30"

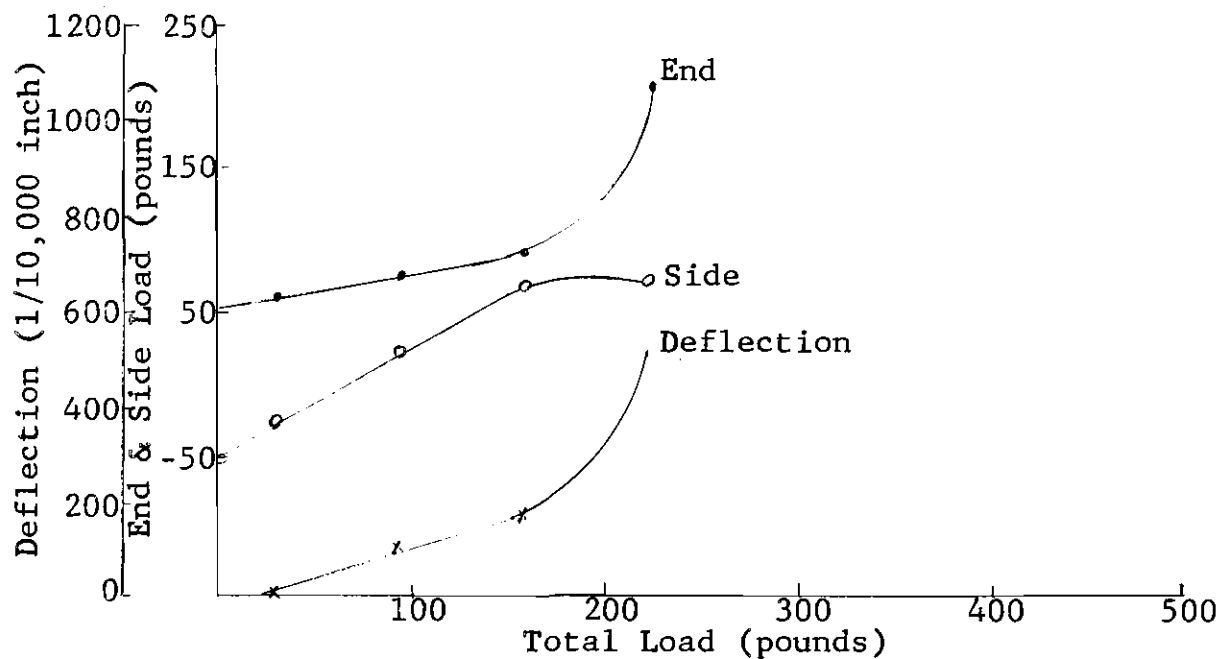


Fig. 7. Pile Load Distribution: Round, Forced, 17"

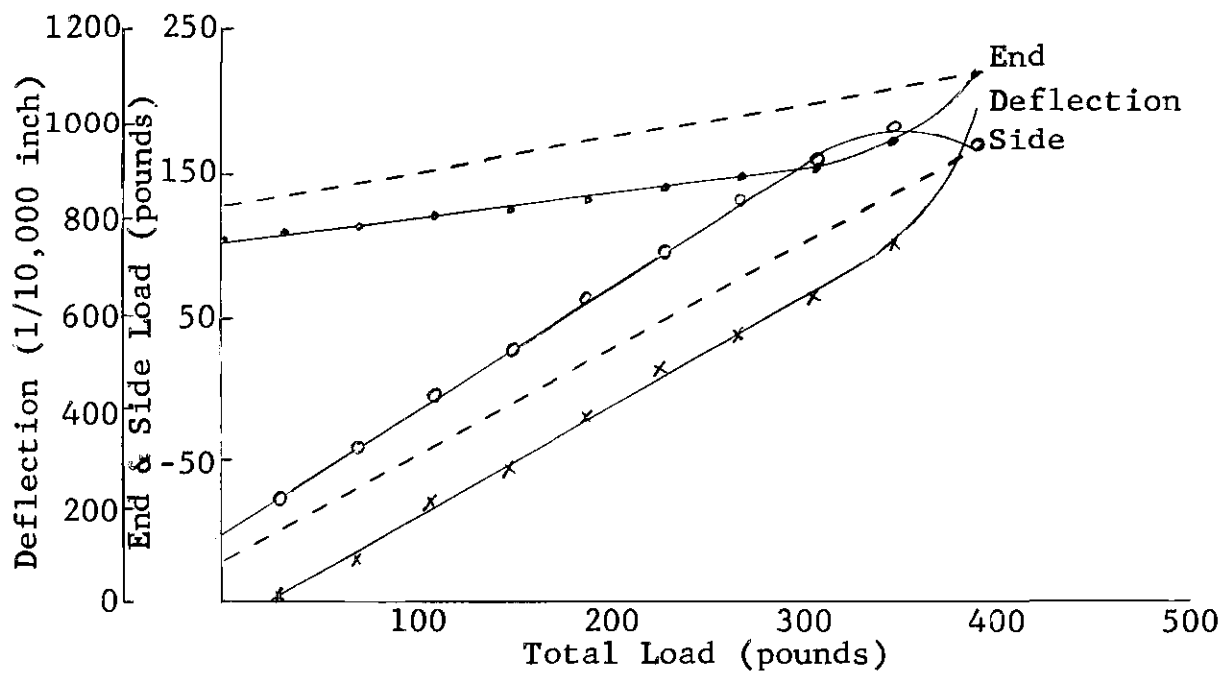


Fig. 8. Pile Load Distribution: Round, Forced, 24"

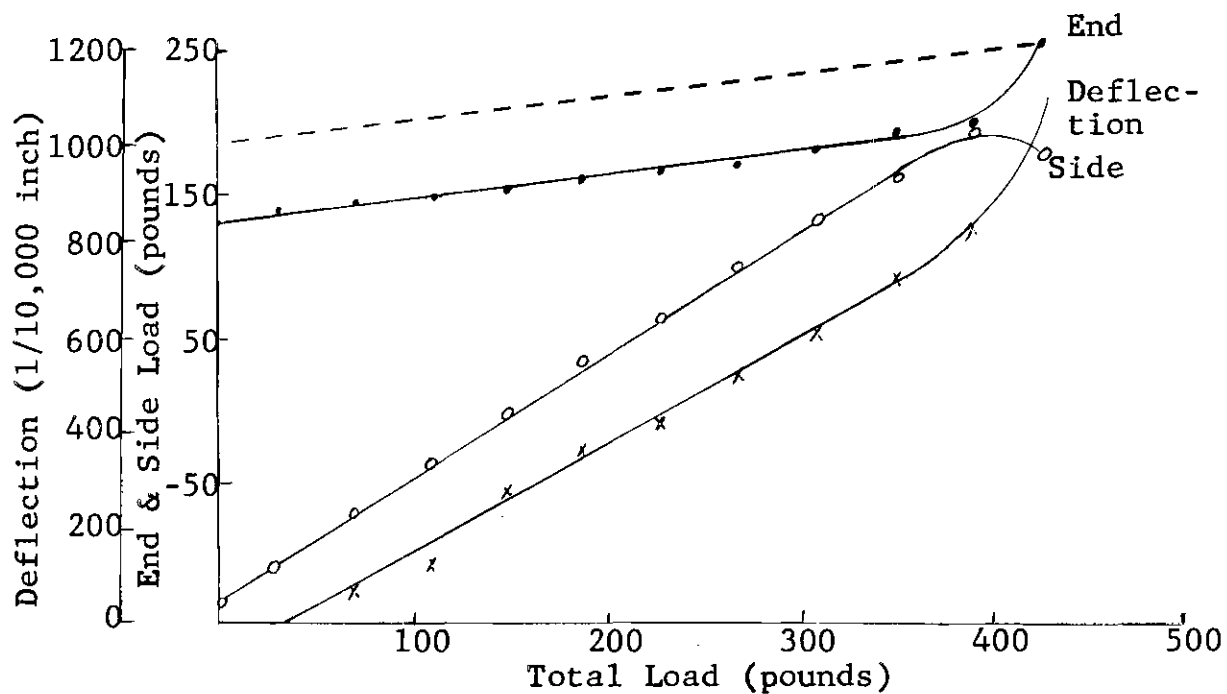


Fig. 9. Pile Load Distribution: Round, Forced, 32"

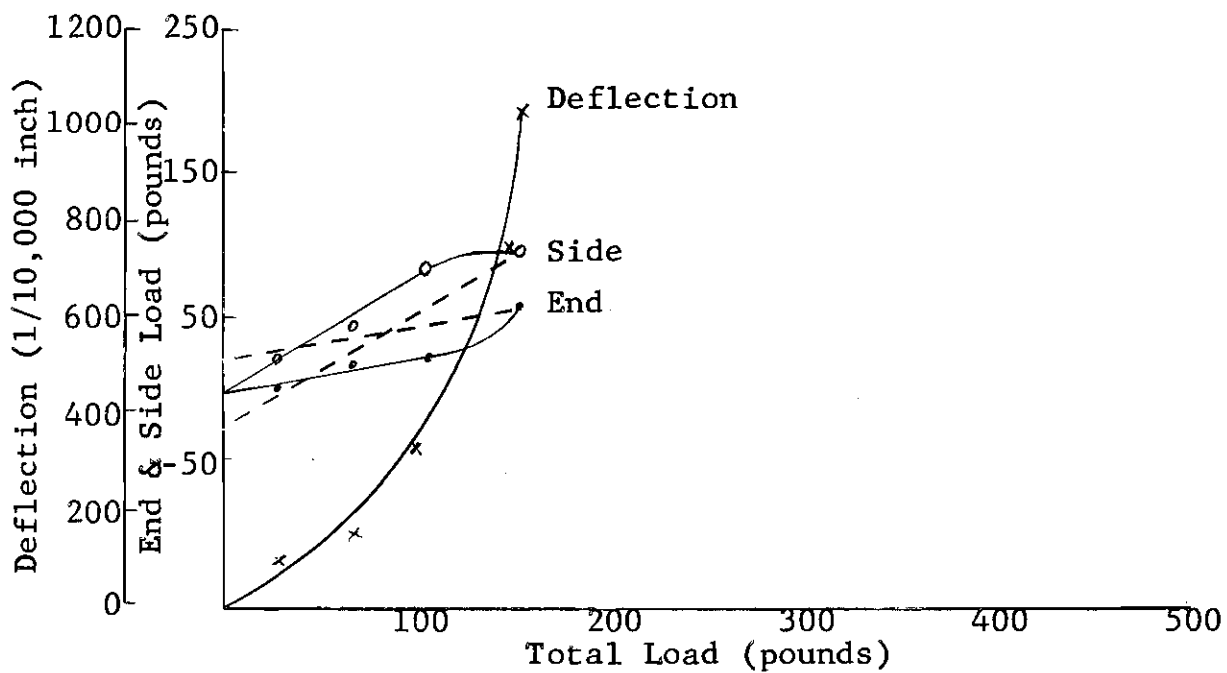


Fig. 10. Pile Load Distribution: Round, Buried, 15"

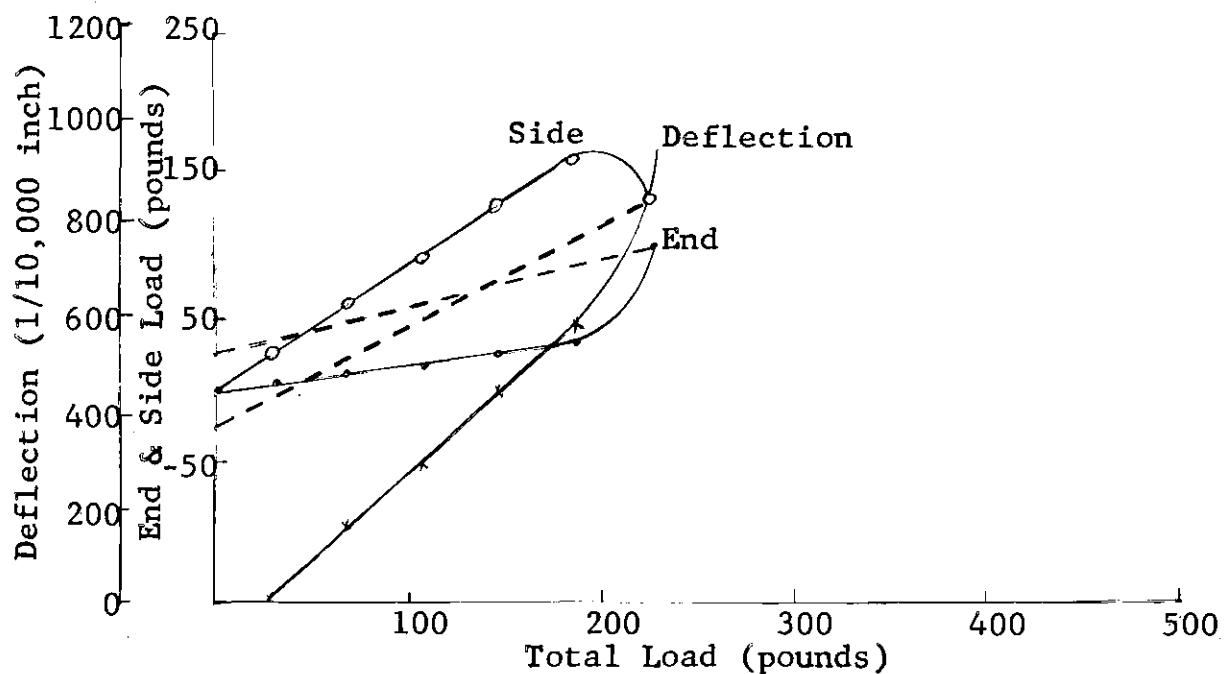


Fig. 11. Pile Load Distribution: Round, Buried, 22"

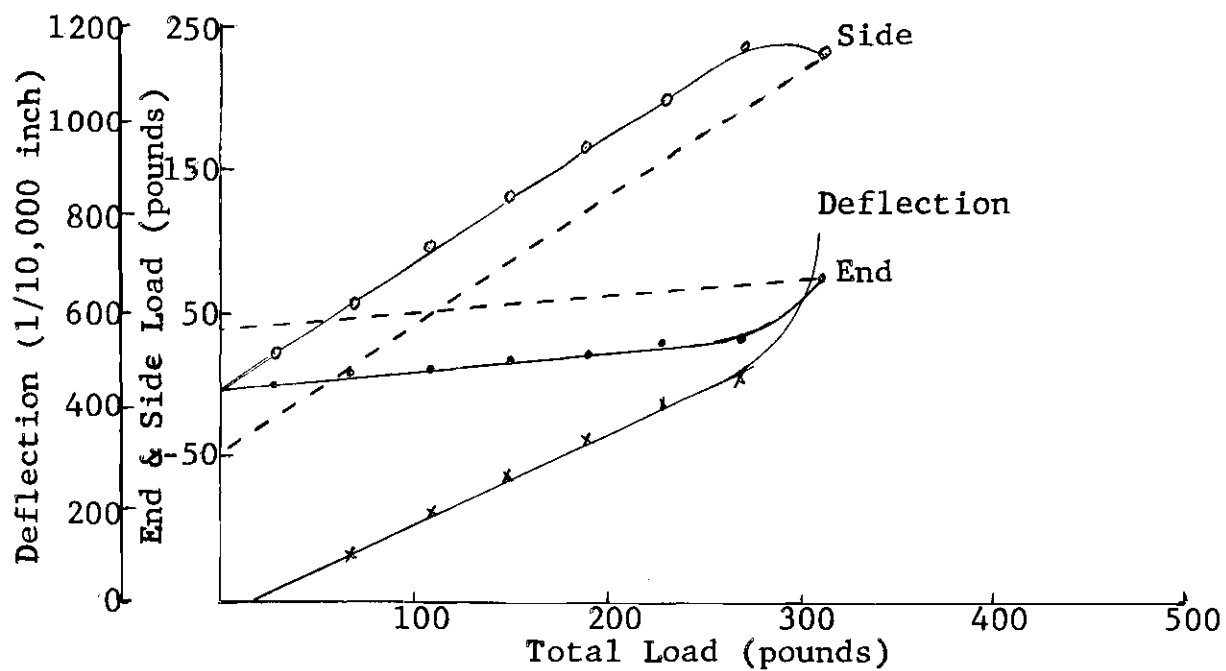


Fig. 12. Pile Load Distribution: Round, Buried, 30"

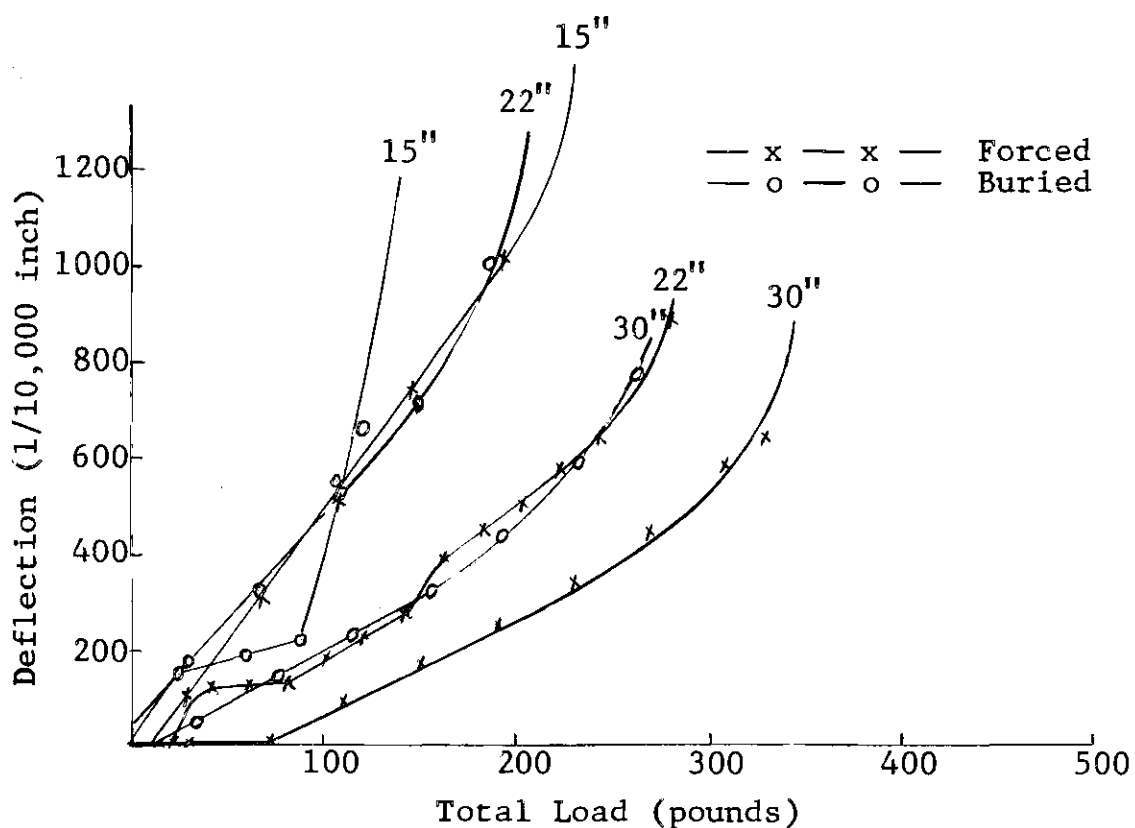


Fig. 13. Deflection of Square Pile Model

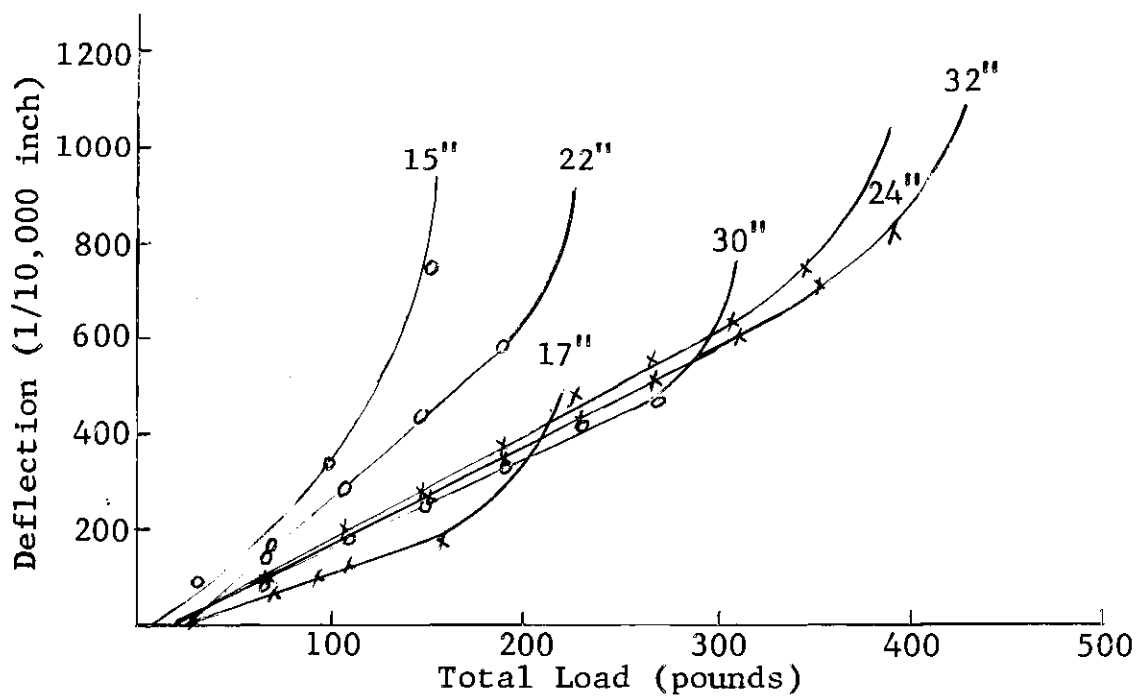


Fig. 14. Deflection of Round Pile Model

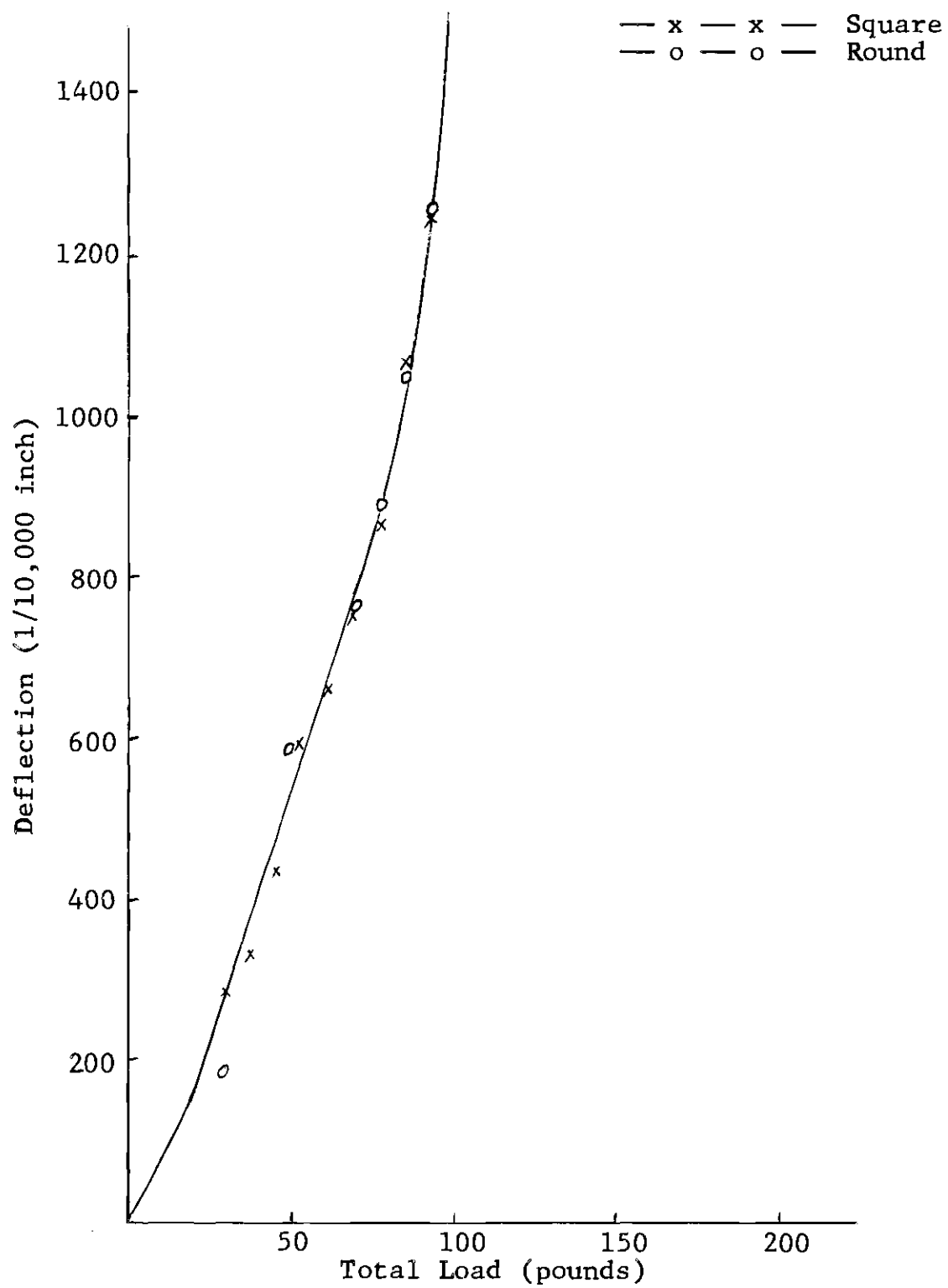


Fig. 15. Plate Load Tests: Round and Square Bases

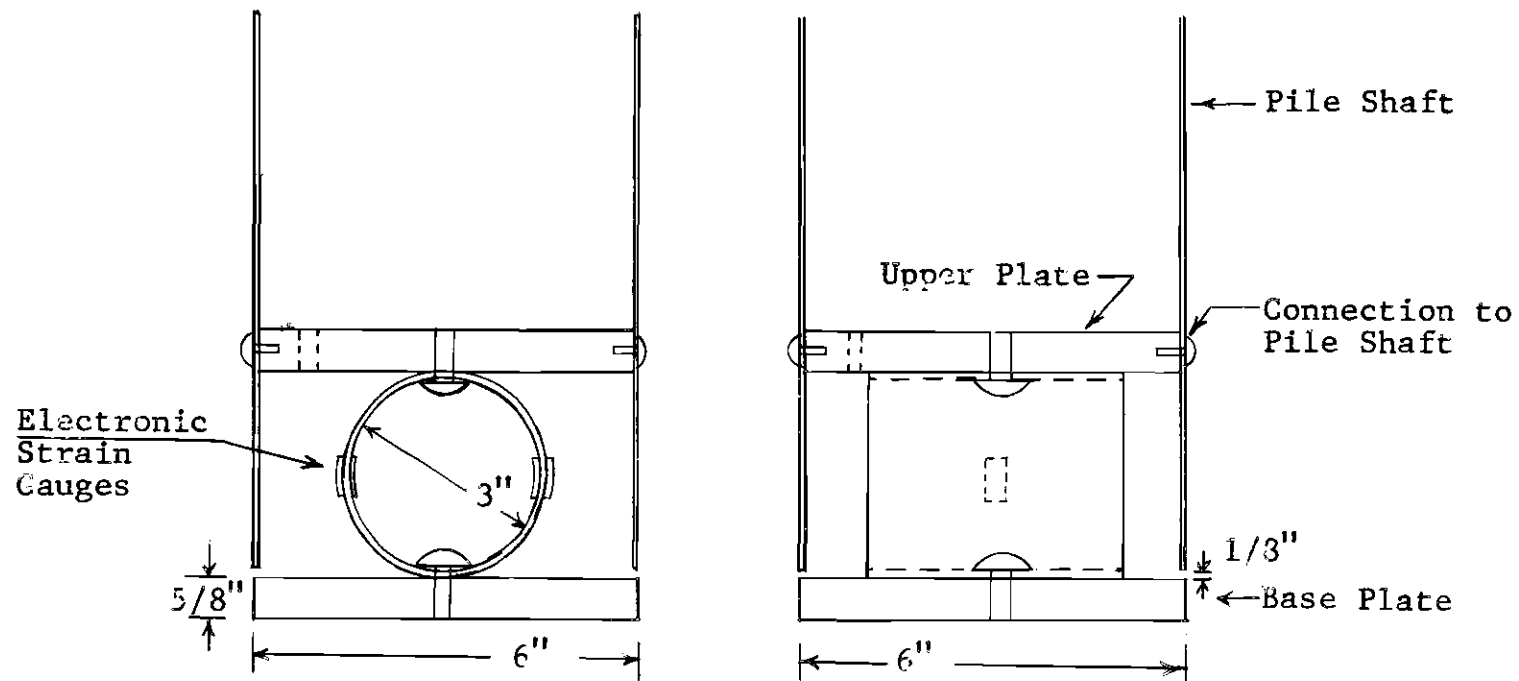


Fig. 16. Diagram of Stress Measuring Device in Pile Base

Table 1. Square Pile Model--Forced Embedment
(Data Sheet)

Depth of Embedment (inches)	Total Load (pounds)	Deflection (inches)	Strain Gauge #1 (inches)	Strain Gauge #2 (inches)
0	0	--	0	0
15	0	--	1,120	1,065
15*	0	0	750	705
15	29	0.0100	790	725
15	69	0.0312	876	820
15	109	0.0550	980	925
15	149	0.0705	1,110	1,060
15	189	0.1020	1,255	1,210
15	229	failure	1,580	1,565
15	0	--	985	935
22	0	--	1,530	1,490
22*	0	0	1,105	1,054
22	20	0	1,135	1,080
22	40	0.0120	1,165	1,115
22	60	0.0120	1,195	1,145
22	80	0.0125	1,230	1,185
22	100	0.0190	1,270	1,220
22	120	0.0225	1,300	1,255
22	140	0.0270	1,345	1,285
22	160	0.0390	1,375	1,330
22	180	0.0440	1,420	1,375
22	200	0.0498	1,470	1,425
22	220	0.0580	1,515	1,470
22	240	0.0645	1,562	1,520
22	260	0.0770	1,620	1,580
22	280	0.0885	1,760	1,700
22	290	failure	1,950	1,955
22	0	--	1,345	1,340
30	0	--	1,780	1,787
30*	0	0	1,299	1,300
30	32	0.0002	1,338	1,337
30	72	0.0004	1,386	1,388
30	112	0.0091	1,440	1,445
30	152	0.0170	1,498	1,505
30	192	0.0262	1,553	1,565
30	232	0.0342	1,620	1,628
30	272	0.0442	1,685	1,700
30	312	0.0582	1,772	1,785
30	332	0.0742	1,870	1,890

Table 1. Continued

Depth of Embedment (inches)	Total Load (pounds)	Deflection (inches)	Strain Gauge #1 (inches)	Strain Gauge #2 (inches)
30	340	0.0922	1,940	1,960
30	348	failure	2,090	2,155
30	0	--	1,602	1,633

*Plus 3 days.

Shear value = 30 inch-pounds
Sensitivity = 2

Table 2. Square Pile Model--Buried Embedment
(Data Sheet)

Depth of Embedment (inches)	Total Load (pounds)	Deflection (inches)	Strain Gauge #1 (inches)	Strain Gauge #2 (inches)
15	0	0	0	0
15	23	0.0140	30	38
15	55	0.0182	77	85
15	87	0.0215	130	141
15	119	0.0655	189	191
15	151	0.1470	515	522
15	183	0.2340	905	913
15	215	failure	1,315	1,248
15	0	--	860	858
22	0	0	0	0
22	29	0.0168	60	50
22	69	0.0320	130	115
22	109	0.0508	210	190
22	149	0.0740	290	275
22	189	0.1000	390	365
22	229	failure*	660	665
22	237	0.2240	810	825
22	257	0.3930	1,120	1,125
22	0	--	665	600
30	0	0	0	0
30	32	0.0050	40	35
30	72	0.0135	85	90
30	112	0.0220	135	145
30	152	0.0320	195	200
30	192	0.0440	255	260
30	232	0.0575	325	340
30	272	failure	625	610
30	292	--	1,095	1,110
30	0	--	855	870

*Partial.

Table 3. Square Pile Model--Forced Embedment
(Load Distribution)

Depth of Embedment (inches)	Total Load (pounds)	Average End Load (pounds)	Side Load (pounds)
15	0	95	-95
15	0*	64	-64
15	29	68	-39
15	69	75	-6
15	109	84	25
15	149	96	53
15	189	109	80
15	229	139	90
15	0	84	-84
22	0	135	-135
22	0*	98	-98
22	20	101	-81
22	40	104	-64
22	60	107	-47
22	80	110	-30
22	100	113	-13
22	120	116	4
22	140	119	21
22	160	122	38
22	180	125	55
22	200	130	70
22	220	134	86
22	240	139	101
22	260	144	116
22	280	156	124
22	290	174	116
22	0	119	-119
30	0	159	-159
30	0*	116	-116
30	32	119	-87
30	72	123	-51
30	112	128	-16
30	152	133	19
30	192	139	53
30	232	144	88
30	272	150	122
30	312	158	154
30	332	168	164
30	340	174	166

Table 3. Continued

Depth of Embedment (inches)	Total Load (pounds)	Average End Load (pounds)	Side Load (pounds)
30	348	189	159
30	0	123	-123

*Plus 3 days.

Table 4. Square Pile Model--Buried Embedment
(Load Distribution)

Depth of Embedment (inches)	Total Load (pounds)	Average End Load (pounds)	Side Load (pounds)
15	0	0	0
15	23	4	19
15	55	8	47
15	87	12	75
15	119	17	102
15	151	45	106
15	183	82	101
15	215	112	103
15	0	75	-75
22	0	0	0
22	29	5	24
22	69	11	58
22	109	18	91
22	149	24	125
22	189	31	158
22	229	57	172
22	237	73	164
22	257	100	157
22	0	55	-55
30	0	0	0
30	32	2	30
30	72	7	65
30	112	11	101
30	152	17	135
30	192	22	170
30	232	30	202
30	272	55	217
30	292	99	193
30	0	77	-77

Table 5. Round Pile Model--Forced Embedment
(Data Sheet)

Depth of Embedment (inches)	Total Load (pounds)	Deflection (inches)	Strain Gauge #1 (inches)	Strain Gauge #2 (inches)
0	0	--	0	0
17	0	--	770	635
17*	0	0	620	510
17	29	0	670	560
17	93	0.0096	825	705
17	158	0.0169	1,029	897
17	222	failure	1,720	1,555
24	0	--	1,455	1,280
24*	0	0	1,165	1,005
24	29	0.0010	1,205	1,040
24	69	0.0085	1,260	1,095
24	109	0.0205	1,320	1,150
24	149	0.0275	1,390	1,215
24	189	0.0380	1,465	1,285
24	229	0.0480	1,545	1,357
24	269	0.0550	1,625	1,435
24	309	0.0630	1,720	1,725
24	349	0.0740	1,890	1,725
24	389	failure	2,450	2,230
24	0	--	1,395	1,205
32	0	--	1,980	1,710
32*	0	0	1,515	1,300
32	29	0	1,560	1,343
32	69	0.0065	1,610	1,385
32	109	0.0120	1,670	1,440
32	149	0.0275	1,735	1,495
32	189	0.0355	1,810	1,560
32	229	0.0415	1,880	1,620
32	269	0.0515	1,950	1,685
32	309	0.0600	2,046	1,765
32	349	0.0715	2,200	1,835
32	389	0.0825	2,275	1,935
32	429	failure	2,800	2,595
32	0	--	2,090	1,795

*Minus 3 days.

Table 6. Round File Model--Buried Embedment
(Data Sheet)

Depth of Embedment (inches)	Total Load (pounds)	Deflection (inches)	Strain Gauge #1 (inches)	Strain Gauge #2 (inches)
15	0	0	0	0
15	29	0.0100	51	44
15	69	0.0150	146	137
15	109	0.0335	256	252
15	149	0.0755	541	552
15	157	0.1030	646	637
15	0	--	281	277
22	0	0	0	0
22	29	0	45	40
22	69	0.0160	110	100
22	109	0.0290	177	158
22	149	0.0440	255	223
22	189	0.0580	335	290
22	229	failure	1,045	960
22	0	--	670	595
30	0	0	0	0
30	29	0	30	35
30	69	0.0095	110	110
30	109	0.0180	140	140
30	149	0.0255	195	195
30	189	0.0335	245	240
30	229	0.0415	290	290
30	269	0.0460	350	350
30	309	failure	770	810
30	0	--	445	430

Shear Value = 29.7 inch-pounds

Table 7. Round Pile Model--Forced Embedment
(Load Distribution)

Depth of Embedment (inches)	Total Load (pounds)	Average End Load (pounds)	Side Load (pounds)
17	0	66	-66
17	0*	53	-53
17	29	58	-29
17	93	72	21
17	158	91	67
17	222	153	69
24	0	128	-128
24	0*	102	-102
24	29	106	-77
24	69	110	-41
24	109	117	-8
24	149	122	27
24	189	129	60
24	229	136	93
24	269	144	125
24	309	152	157
24	349	170	179
24	389	221	168
24	0	122	-122
32	0	174	-174
32	0*	132	-132
32	29	137	-108
32	69	141	-72
32	109	146	-37
32	149	152	-3
32	189	159	30
32	229	165	64
32	269	171	98
32	309	179	130
32	349	190	159
32	389	199	190
32	429	254	175
32	0	183	-183

*Minus 3 days.

Table 8. Round Pile Model--Buried Embedment
(Load Distribution)

Depth of Embedment (inches)	Total Load (pounds)	Average End Load (pounds)	Side Load (pounds)
15	0	0	0
15	29	5	24
15	69	14	55
15	109	23	86
15	149	50	99
15	157	59	98
15	0	25	-25
22	0	0	0
22	29	4	25
22	69	10	59
22	109	17	92
22	149	25	124
22	189	30	159
22	229	97	132
22	0	59	-59
30	0	0	0
30	29	3	26
30	69	10	59
30	109	13	96
30	149	18	131
30	189	23	166
30	229	28	201
30	269	33	236
30	309	75	234
30	0	41	-41

Table 9. Plate Load Test Results

Plate Type	Plate Area (square inches)	Load (pounds)	Deflection (inches)
Square	25.0	0	0
Square	25.0	30	0.0286
Square	25.0	38	0.0336
Square	25.0	46	0.0436
Square	25.0	54	0.0594
Square	25.0	62	0.0664
Square	25.0	70	0.0751
Square	25.0	78	0.0866
Square	25.0	86	0.1066
Square	25.0	94	0.1246
Square	25.0	102	0.1556
Square	25.0	110	0.1876
Square	25.0	0	0.0566
Round	28.3	0	0
Round	28.3	30	0.0188
Round	28.3	50	0.0590
Round	28.3	70	0.0770
Round	28.3	78	0.0890
Round	28.3	86	0.1050
Round	28.3	94	0.1260
Round	28.3	102	0.1590
Round	28.3	110	0.1780
Round	28.3	118	0.2185
Round	28.3	0	0.0995

Table 10. Summary of Soil Test Results

-
1. Undrained shear strength (vane shear) = 0.955 psi
(square pile--forced)
 2. Undrained shear strength (vane shear) = 0.945 psi
(round pile--buried)
 3. Adhesion: plastic-clay (plate test) = 0.885 psi
 4. Adhesion: plastic-clay (pile rotation) = 0.705 psi
 5. Unit weight of bentonite = 2,435 grams per liter or 152
pounds per cubic foot
-

Table 10-a. Soil Properties Used in Calculations

-
1. Average undrained shear strength of bentonite = 0.950 psi
 2. Adhesion of bentonite to plastic coated metal = 0.705 psi
 3. Unit weight of bentonite = 152 pounds per cubic foot
-

Table 11. Calculated Bearing Capacities

Bearing capacities are calculated according to Equation (4):

$$Q = (cN_c + \gamma D)A + mS$$

Constants used through the following calculations are:

$$c = 0.950 \text{ pounds per square inch}$$

$$N_c = 9 \quad (\text{except for plate load tests where } N_c = 6.2)$$

$$\gamma = 152 \text{ pounds per cubic foot}$$

$$m = 0.705 \div 0.950 = 0.742$$

1. Plate Load Tests:

- a. Square pile base-- $D = 0.0$; $A = 25.0$ square inches; $S = 0$

$$Q = 147 \text{ pounds}$$

- b. Round pile base-- $D = 0.0$; $A = 27.7$ square inches; $S = 0$

$$Q = 163 \text{ pounds}$$

2. Square Pile:

- a. Embedded 15"-- $D = 15''$; $A = 25.0$ square inches; $S = 300$ square inches

$$Q = 247 + 212 = 459 \text{ pounds}$$

- b. Embedded 22"-- $D = 22''$; $A = 25.0$ square inches; $S = 440$ square inches

$$Q = 262 + 310 = 572 \text{ pounds}$$

- c. Embedded 30"-- $D = 30''$; $A = 25.0$ square inches; $S = 600$ square inches

$$Q = 290 + 423 = 713 \text{ pounds}$$

Table 11. Continued

3. Round Pile:

- a. Embedded 17"--D = 17"; A = 27.7 square inches; S = 318 square inches

$$Q = 278 + 224 = 502 \text{ pounds}$$

- b. Embedded 24"--D = 24"; A = 27.7 square inches; S = 449 square inches

$$Q = 295 + 316 = 611 \text{ pounds}$$

- c. Embedded 32"--D = 32"; A = 27.7 square inches; S = 598 square inches

$$Q = 315 + 422 = 737 \text{ pounds}$$

- d. Embedded 15"--D = 15"; A = 27.7 square inches; S = 280 square inches

$$Q = 273 + 197 = 470 \text{ pounds}$$

- e. Embedded 22"--D = 22"; A = 27.7 square inches; S = 411 square inches

$$Q = 291 + 290 = 581 \text{ pounds}$$

- f. Embedded 30"--D = 30"; A = 27.7 square inches; S = 561 square inches

$$Q = 310 + 395 = 705 \text{ pounds}$$

Table 12. Comparative Bearing Capacities

	Calculated (pounds)	Measured (pounds)	% Measured of Calculated
1. Plate (square)	147	85	58
2. Plate (round)	163	86	53
3. Pile (sq. F, 15")			
a. End	247	110	45
b. Friction	212	80	38
c. Total	459	190	41
4. Pile (sq. B, 15")			
a. End	247	18	7
b. Friction	212	107	51
c. Total	459	125	27
5. Pile (sq. F, 22")			
a. End	262	150	57
b. Friction	310	125	40
c. Total	572	275	48
6. Pile (sq. B, 22")			
a. End	262	56	21
b. Friction	310	164	53
c. Total	572	220	39
7. Pile (sq. F, 30")			
a. End	290	170	59
b. Friction	423	165	39
c. Total	713	335	47
8. Pile (sq. B, 30")			
a. End	290	52	18
b. Friction	423	218	52
c. Total	713	270	38
9. Pile (rd. F, 17")			
a. End	278	90	32
b. Friction	224	68	32
c. Total	502	158	32

Table 12. Continued

	Calculated (pounds)	Measured (pounds)	% Measured of Calculated
10. Pile (rd. B, 15")			
a. End	273	28	10
b. Friction	197	92	47
c. Total	470	120	26
11. Pile (rd. F, 24")			
a. End	295	170	58
b. Friction	316	178	56
c. Total	611	348	57
12. Pile (rd. B, 22")			
a. End	291	30	10
b. Friction	290	160	55
c. Total	581	190	33
13. Pile (rd. F, 32")			
a. End	315	200	64
b. Friction	422	190	45
c. Total	737	390	53
14. Pile (rd. B, 30")			
a. End	310	35	11
b. Friction	395	235	60
c. Total	705	270	38

Table 13. Average Efficiency*

1. Square pile, end, forced	54%
2. Square pile, friction, forced	39%
3. Square pile, friction, buried	43%
4. Square pile, end, buried	15%
5. Round pile, end, forced	51%
6. Round pile, friction, forced	44%
7. Round pile, end, buried	10%
8. Round pile, friction, buried	51%

*Per cent measured of calculated strength.

Table 14. Residual Side Friction
(Forced Piles After Three Days)

1. Square, F, 15"	0.214 psi
2. Square, F, 22"	0.222 psi
3. Square, F, 30"	0.265 psi

Average square 0.234 psi

4. Round, F, 17"	0.167 psi
5. Round, F, 24"	0.227 psi
6. Round, F, 32"	0.235 psi

Average round (less No. 4) 0.231

All 0.233

Table 15. Measured Skin Friction

Test	Side Friction (pounds)	Surface Area (sq. inches)	Skin Friction (psi)
1. Sq. F, 15"	80	300	0.267
2. Sq. F, 22"	125	440	0.284
3. Sq. F, 30"	165	600	0.275
4. Sq. B, 15"	107	300	0.357
5. Sq. B, 22"	164	440	0.372
6. Sq. B, 30"	218	600	0.364
7. Rd. F, 17"	68	318	0.214
8. Rd. F, 24"	178	449	0.396
9. Rd. F, 32"	190	598	0.318
10. Rd. B, 15"	92	280	0.328
11. Rd. B, 22"	160	411	0.390
12. Rd. B, 30"	235	561	0.419

Average square piles 0.320 psi
 Average round piles 0.370 psi (omitting rd. F, 17")
 Average forced piles 0.292 psi
 Average buried piles 0.372 psi
 Overall average 0.332 psi

Table 16. Modification of Bearing Capacities of Round Piles (Forced) to Compare with Standard Depth

Pile Model	Skin Friction (psi)	Friction from Additional 2" (pounds)	Measured Bearing Capacity (pounds)	Comparative Bearing Capacity (pounds)
Rd. F, 17"	0.214	8.0	158	150
Rd. F, 24"	0.396	14.8	348	333
Rd. F, 32"	0.318	11.8	390	378

BIBLIOGRAPHY

LITERATURE CITED

1. Meyerhoff, G. G. and L. J. Murdock, "An Investigation of the Bearing Capacity of Some Bored and Driven Piles in Londod Clay," Geotechnique, Vol. 3, No. 4. London: Hollen Street Press, Ltd., 1953, pp. 267-282.
2. Ibid., p. 279.
3. Solomon, John W., "Timber Friction Pile Foundations - Discussion," Proceedings, American Society of Civil Engineers, Vol. 68, June 1942, pp. 1044-1046.
4. Seed, H. Bolton and Lyman C. Reese, "The Action of Soft Clay Along Friction Piles," Transactions, A.S.C.E., Vol. 122, 1957, pp. 735-737.
5. Chellis, R. D., Pile Foundations: Theory, Design, Practice. New York: McGraw-Hill, 1951, p. 42.
6. Ibid., p. 45.
7. Ibid., p. 49.
8. Martin, Carl Bernard, Model Studies of the Bearing Capacity of File Groups in a Saturated Clay. Unpublished M.S. thesis, School of Civil Engineering, Georgia Institute of Technology, 1957, p. 11.
9. Wilson, Lyle Lawrence, Model Studies of the Load Distribution Within Groups of Friction Piles In a Cohesive Soil. Unpublished M.S. thesis, School of Civil Engineering, Georgia Institute of Technology, 1957, p. 20.